

Research Article

Hongmei Gao, Zhaohui Guo*

LncRNA XIST regulates atherosclerosis progression in ox-LDL-induced HUVECs

<https://doi.org/10.1515/med-2021-0200>

received January 16, 2020; accepted November 12, 2020

Abstract: Long noncoding RNAs (lncRNAs) have been verified as vital regulators in human disease, including atherosclerosis. However, the precise role of X-inactive-specific transcript (XIST) in atherosclerosis remains unclear. The proliferation and apoptosis of human umbilical vein endothelial cells (HUVECs) exposed to low-density lipoprotein (ox-LDL) were assessed by 3-(4,5-dimethylthiazol-2-yl)-2,5-diphenyl-2H-tetrazol-3-ium bromide, and flow cytometry assays, correspondingly. The western blot assay was used to quantify protein expression. Lactate dehydrogenase activity and the concentrations of inflammatory factors were measured by matched kits. The real-time quantitative polymerase chain reaction (qPCR) was used to determine α -smooth muscle actin, smooth muscle protein 22- α , XIST, miR-98-5p, and pregnancy-associated plasma protein A (PAPPA) levels in HUVECs. The relationship among XIST, miR-98-5p, and PAPPA was analyzed by dual-luciferase reporter, RNA immunoprecipitation, and RNA pull-down assays. We found ox-LDL repressed proliferation and induced inflammation and apoptosis in HUVECs. Loss-of-functional experiment suggested that the down-regulation of XIST overturned the ox-LDL-induced effects on HUVECs. Additionally, overexpression of miR-98-5p-induced effects on ox-LDL-stimulated HUVECs was abolished by upregulation of XIST. However, silencing of miR-98-5p strengthened the ox-LDL-induced effects on HUVECs by increasing expression of PAPPA. Mechanistically, XIST could regulate PAPPA expression in ox-LDL-induced HUVECs by sponging miR-98-5p, providing understanding for atherosclerosis.

Keywords: XIST, miR-98-5p, PAPPA, ox-LDL, HUVECs

* **Corresponding author: Zhaohui Guo**, Department of Neurology, The Fourth Affiliated Hospital of Harbin Medical University, No. 37 Yiyuan Street, Nangang District, 150001, Harbin, Heilongjiang, China, e-mail: guozhaohui_79@163.com, tel: +86-139-3629-0943
Hongmei Gao: Department of Neurology, The Fourth Affiliated Hospital of Harbin Medical University, No. 37 Yiyuan Street, Nangang District, 150001, Harbin, Heilongjiang, China

1 Introduction

Atherosclerosis is the most common cause of cerebrovascular disease and is a complex polygenic disease with high mortality [1], while its pathogenesis has not been fully understood [2]. Oxidized low-density lipoprotein (ox-LDL) is a foremost inducer for atherosclerosis [3]. ox-LDL could enhance proliferation and invasion of vascular smooth muscle cells (VSMCs) [4]; meanwhile, several investigations have demonstrated that ox-LDL promoted the apoptosis of human umbilical vein endothelial cells (HUVECs) and regulated the activity of caspase 3 and caspase 9. Conclusively, ox-LDL played critical roles in the pathogenesis of cerebrovascular disease [5,6].

Although noncoding property, long noncoding RNAs (lncRNAs), more than 200 nucleotides in length, were implicated in numerous biological behaviors by regulation of gene expression [7]. Moreover, accumulating evidence suggested the lncRNAs played key roles in atherosclerosis, implicating proliferation and apoptosis of smooth muscle and endothelial cells, inflammation, and lipid metabolism [8,9]. Increasing evidence has confirmed that XIST was increased in various human diseases, including nasopharyngeal carcinoma [10], glioblastoma [11], and lung cancer [12]. Additionally, XIST was overexpressed in human brain microvascular endothelial cells exposed to hypoxia [13]. Nevertheless, the regulatory mechanism of XIST was unidentified in atherosclerosis.

MiRNAs, noncoding RNAs and key mediators in diverse biological pathways, could control cellular activity under pathologic situations, including atherosclerosis [14]. Therefore, mechanistic dissection of miRNA functions may help us to comprehend the roles of miRNAs in disease, which promoted the development of miRNA-based therapeutics [15]. Sun et al. and Li et al. confirmed that miR-98 protected myocardium cells or endothelial cells against myocardial infarction or hypoxia/reoxygenation-induced apoptosis by targeting caspase-3, respectively, indicating that miRNA-98 was a stress-specific miRNA participating in cell survival and apoptosis [16,17]. However, the mechanism of miR-98-5p in ox-LDL-stimulated HUVECs remains unknown.

Pregnancy-associated plasma protein A (PAPPA), a zinc metalloproteinase, played significant roles in atherosclerosis [18]. The elevated PAPPA level was a poor prognosis factor in vascular diseases [19]. Therefore, the role of PAPPA in atherosclerosis was worth investigating. In this study, the influences of ox-LDL in proliferation, inflammation, and apoptosis of HUVECs, as well as XIST, miR-98-5p, and PAPPA in HUVECs under ox-LDL administration, were investigated.

2 Materials and methods

2.1 Cell lines and cell culture

HUVECs were bought from American Type Culture Collection (Rockville, MD, USA) and cultured in DMEM medium (GIBCO BRL, Grand Island, NY, USA) supplemented with 10% fetal bovine serum (FBS; GIBCO BRL), 100 µg/mL of streptomycin, and 100 U/mL of penicillin (GIBCO BRL). Cells were cultivated in standard culture conditions (5% CO₂, 37°C). Ox-LDL (Sigma, St. Louis, MO, USA) was used to culture cells to establish an arteriosclerosis stimulation for HUVECs. The usage of HUVECs was approved by the Ethics Committee of Fourth Affiliated Hospital of Harbin Medical University.

2.2 3-(4,5-Dimethylthiazol-2-yl)-2,5-diphenyl-2H-tetrazol-3-ium bromide (MTT) assay

Cell viability was tested by MTT assay. In brief, 2.0×10^3 HUVECs were sowed into 96 wells and allowed to adhere. After incubation for indicated times, 10 µL of 5 mg/mL MTT (Beyotime, Jiangsu, China) solution was added to each well of the 96 wells plate and allowed to incubate for additional 4 h. The supernatant was replaced by 150 µL of dimethyl sulfoxide (DMSO) and then shocked for 10 min. The absorbance was detected at 490 nm under a microplate spectrophotometer (Olympus, Tokyo, Japan).

2.3 Cell apoptosis assay

Annexin V labeled with fluorescein isothiocyanate (FITC)/propidium iodide (PI) Apoptosis Detection Kit

(Thermo Fisher Scientific, Waltham, MA, USA) was performed for cell apoptosis assay. After treatment, HUVECs were harvested by trypsinization. Then, cells were resuspended with phosphate buffer saline buffer solution into a single cell suspension (1×10^7 /mL). 100 µL of cell suspension was reacted with 5 µL of Annexin V-FITC and 5 µL of PI in the dark condition. The apoptotic cells were measured using flow cytometer (Applied Biosystems, Foster City, CA, USA) and the Flowjo V10 software (Tree Star, San Francisco, CA, USA) was used to quantify the results.

2.4 Western blot assay

Radio-immunoprecipitation assay buffer (Beyotime) containing protease inhibitors was used to extract proteins from HUVECs at 4°C. In addition, protein concentrations were checked with a bicinchoninic acid (BCA) protein assay (Solarbio, Beijing, China). Proteins were fractionated on 12% sodium dodecyl sulfate polyacrylamide gel electrophoresis, and then electroblotted onto the polyvinylidene difluoride membranes (GE Healthcare, Piscataway, NJ, USA). After being blocked with 3% Albumin Bovine V (Amyjet scientific, Wuhan, China), the membranes were interacted with the indicated antibodies. After being washed, membranes were incubated with the Goat polyclonal Secondary Antibody to Rabbit IgG-H&L (ab150077; 1:2,000 dilution; Abcam, Cambridge, MA, USA) for 2 h. Eventually, the western blot bands were visualized by ECL Western Blotting Detection Kit (Solarbio) under Alpha Innotech Imaging System (Protein Simple, Santa Clara, CA, USA). The related protein expression was standardized to β-actin. The primary antibodies were listed: anti-BCL2-Associated X (Bax; ab32503; 1:1,000 dilution; Abcam), anti-B-cell lymphoma-2 (Bcl-2; ab32124; 1:1,000 dilution; Abcam), anti-α-smooth muscle actin (α-SMA; ab5694; 1:1,000 dilution; Abcam), anti-smooth muscle protein 22-α (SM22-α; ab14106; 1:1,000 dilution; Abcam), anti-PAPPA (ab174314; 1:1,000 dilution; Abcam), and β-actin (ab179467; 1:3,000 dilution; Abcam).

2.5 Measurement of lactate dehydrogenase (LDH)

Cytotoxicity was evaluated by measuring LDH released in the medium after treatment with ox-LDL at different time points using the LDH activity detection kit (Solarbio) as described by Wang et al. [20].

2.6 Enzyme-linked immunosorbent assay (ELISA)

The concentrations of interleukin 6 (IL-6), interleukin 1 β (IL-1 β), and tumor necrosis factor α (TNF- α) in medium were evaluated by IL-6 ELISA KIT, IL-1 β ELISA KIT, and TNF- α ELISA KIT (Boster, Wuhan, China) as instructed by the manufacturer, respectively. The absorbance was measured under a microplate spectrophotometer (Olympus).

2.7 Real-time quantitative polymerase chain reaction (qPCR)

Total RNA was isolated using TriQuick Reagent (Solarbio) in accordance with the producer's procedures. For lncRNA/mRNA, RNA was used to synthesize complementary DNA (cDNA) with a cDNA Reverse Transcription kit (Bio-Rad, Hercules, CA, USA). The expression levels of lncRNA/mRNA were evaluated using Quantitect SYBR Green Kit (Qiagen, Hilden, Germany) based on the $2^{-\Delta\Delta Ct}$ method, with glyceraldehyde-3-phosphate dehydrogenase (GAPDH) as an internal control. For miR-98-5p, cDNA was synthesized and amplified using miScript II RT kit (Qiagen) under Thermal Cycler CFX6 System (Bio-Rad). The expression level of miR-98-5p was standardized to endogenous small nuclear RNA U6.

The sequences of primers used were listed:

α -SMA (Forward-5'-GTCCACCGCAAATGCTTCTAA-3'; Reverse-5'-AAAACACATTAACGAGTCAG-3');
 SM22- α (Forward-5'-TGATTCTGAGCAAGCTGGT-3'; Reverse-5'-TGCCTTCAAAGAGGTCAAC-3');
 XIST (Forward-5'-CTCTCCATTGGGTTTAC-3'; Reverse-5'-GCGGCAGGTCTTAAGAGATGAG-3');
 miR-98-5p (Forward-5'-GCCGAGTGAGGUAGTAAGTTG-3'; Reverse-5'-CTCAACTGGTGTCTGTTGA-3');
 PAPPA (Forward-5'-ACAAAGACCCACGCTACTTTTT-3'; Reverse-5'-CATGAACTGCCATCATAGGTG-3');
 GAPDH (Forward-5'-TCCCATCACCATCTTCCAGG-3'; Reverse-5'-GATGACCCTTTTGGCTCCC-3');
 U6 (Forward-5'-AACGCTTACGAATTTGCGT-3'; Reverse-5'-CTCGCTTCGGCAGCACA-3').

2.8 Transfection assay

Small interfering RNA (siRNA) against XIST (si-XIST) or PAPPA (si-PAPPA) and siRNA scrambled control (si-NC), XIST overexpression vector (pcDNA-XIST), and its negative control (pcDNA) were acquired from GenePharma

(Shanghai, China). MiR-98-5p mimic (miR-98-5p) and control (miR-NC) and miR-98-5p inhibitor (anti-miR-98-5p) and control (anti-NC) were provided by Sangon (Shanghai, China). Different oligonucleotides or vectors were transfected into HUVECs with Lipofectamine 2000 reagent (Qiagen) following the user's guidebook.

2.9 Dual-luciferase reporter assay

We predicted the miR-98-5p binding sites in XIST or 3'untranslated region (UTR) of PAPPA using the bioinformatics database Starbase3.0 (<http://starbase.sysu.edu.cn/>). For the generation of XIST-WT, XIST-MUT, PAPPA 3'UTR-WT, or PAPPA 3'UTR-MUT report vectors, the WT or MUT fragment of XIST and PAPPA 3'UTR were subcloned into the pGL3 vectors (Realgene, Nanjing, China). For the luciferase activity measurement, HUVECs were co-transfected with constructed luciferase reporter vectors according to the experiment design and miR-98-5p mimic or miR-NC. After 48 h, luciferase activity was detected using the Dual-Luciferase Assay Kit (GeneCopoeia, Rockville, MD, USA).

2.10 RNA immunoprecipitation (RIP) assay

The RIP assay was carried out with the Magna RIP RNA-Binding Protein Immunoprecipitation Kit (Sigma) according to manufacturer's instruction. Magnetic beads were pre-conjugated with antibody against Argonaute2 (Ago2; Millipore, Bedford, MA, USA), with IgG as control. HUVECs were collected and then lysed by RIP-buffer, and the lysates were treated with bead antibody complex. After incubation at 4°C overnight, immunoprecipitated RNA was treated with proteinase K buffer and then reverse-transcribed. The abundances of miR-98-5p, PAPPA, and XIST were assessed by qPCR analysis.

2.11 RNA pull-down

The biotin-labeled Bio-miR-98-5p and Bio-NC were synthesized by RiboBio (Guangzhou, China). In brief, 1×10^7 HUVECs were infected with Bio-miR-98-5p or Bio-NC at a final concentration of 50 nM. After 48 h, HUVECs were lysed and incubated with magnetic beads coupled with streptavidin (Life Technologies, Carlsbad, CA, USA). After pulling down, biotin-coupled RNA complex was purified by proteinase K and subjected to qPCR assay.

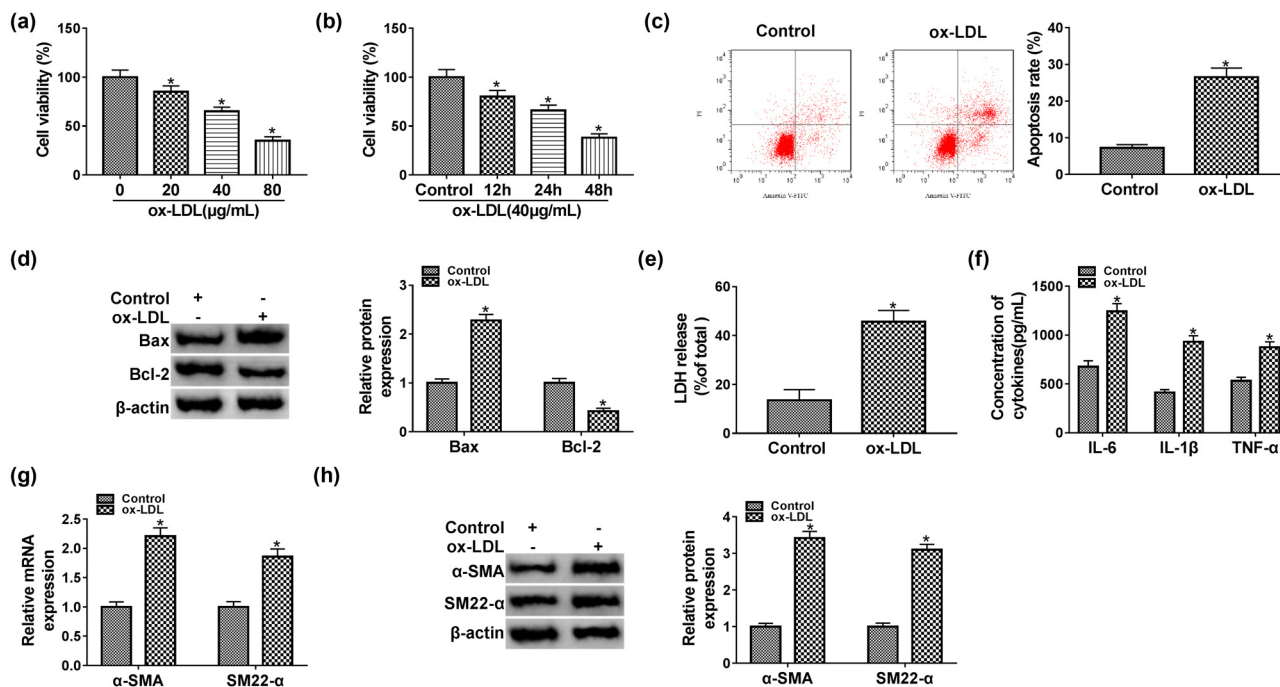


Figure 1: Ox-LDL suppressed proliferation and enhanced apoptosis and inflammatory response in HUVECs. (a and b) The cell viability of HUVECs exposed to ox-LDL was assessed by MTT assay. (c) The flow cytometry assay was performed for examining the apoptosis rate of HUVECs treated with 40 µg/mL of ox-LDL for 48 h. (d) The protein expression levels of Bax and Bcl-2 were measured by western blot assay. (e) LDH release in the medium was examined by a commercial kit. (f) The levels of IL-6, IL-1β, and TNF-α were evaluated in the medium by matched kits. (g and h) The qPCR and western blot assays were used to show the expression levels of α-SMA and SM22-α in HUVECs treated with ox-LDL. Data shown are mean ± SD and from three independent experiments. * $P < 0.05$. Abbreviations: oxidized low-density lipoprotein (ox-LDL), anti-BCL2-Associated X (Bax), anti-B-cell lymphoma-2 (Bcl-2), interleukin 6 (IL-6), interleukin 1β (IL-1β), and tumor necrosis factor α (TNF-α), anti-α-smooth muscle actin (α-SMA), anti-smooth muscle protein 22-α (SM22-α).

2.12 Statistical analysis

The statistics software SPSS 21.0 software (IBM, Somers, NY, USA) was conducted for statistical analysis. The significant differences in selected two groups were determined by Student's *t*-test, while differences of multi-groups were analyzed by one-way analysis of variance (ANOVA) with Turkey's test. $P < 0.05$ was indicated significant differences, and the data were exhibited as mean ± standard deviation.

3 Results

3.1 Ox-LDL inhibited proliferation and induced apoptosis and inflammatory response in HUVECs

Originally, cell viability of HUVECs was assessed by MTT in HUVECs, and the results indicated that cell

viability of HUVECs was declined by ox-LDL in dose/time-dependent manner (Figure 1a and b). Furthermore, apoptosis rate was significantly higher in HUVECs treated with 40 µg/mL of ox-LDL for 48 h compared with control group (Figure 1c). We also measured the expression levels of Bax and Bcl-2 in HUVECs by western blot analysis, and the results revealed that Bax protein level was upregulated, while Bcl-2 was downregulated in HUVECs treated with ox-LDL when compared with control group (Figure 1d). After treatment with 40 µg/mL of ox-LDL for 48 h, the ox-LDL group had the higher LDH release compared with control group (Figure 1e). In ox-LDL condition, inflammatory response was enhanced in HUVECs by upregulating release of inflammatory factors, including IL-6, IL-1β, and TNF-α (Figure 1f). In addition, the mRNA and protein expression levels of α-SMA and SM22-α were upregulated in HUVECs exposed to ox-LDL (Figure 1g and h). In summary, Ox-LDL promoted inflammatory response and apoptosis, as well as suppressed proliferation in HUVECs.

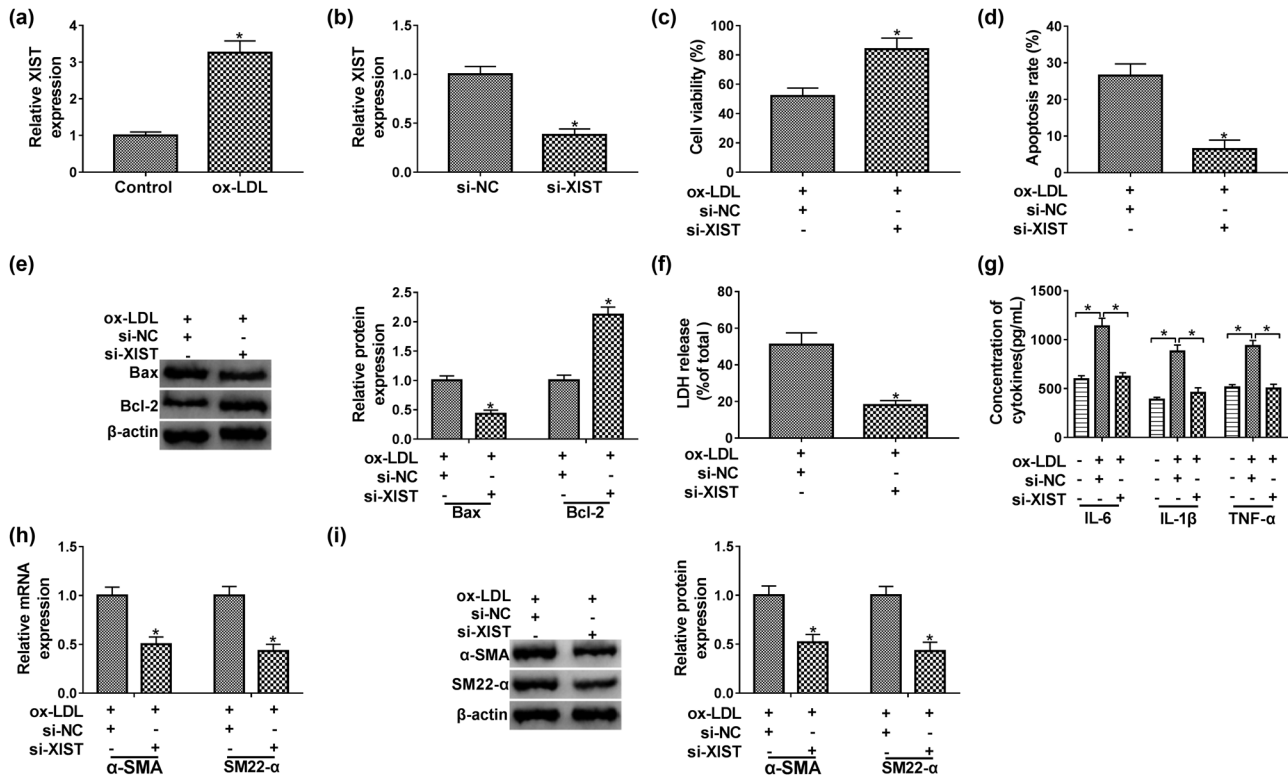


Figure 2: Knockdown of XIST weakened ox-LDL-induced effects on HUVECs. (a) The expression level of XIST in HUVECs treated with ox-LDL was determined by qPCR analysis. (b) The interference efficiency of si-XIST in HUVECs was assessed by qPCR assay. (c–f) HUVECs were divided into two groups: ox-LDL + si-NC and ox-LDL + si-XIST groups. (c) The proliferation capability of HUVECs was measured using MTT assay. (d) The flow cytometry assay was recruited to monitor the apoptosis of HUVECs. (e) The western blot analysis was applied to assess Bax and Bcl-2 expression in HUVECs. (f) A commercial available kit was used to assess LDH release in HUVECs supernatants. (g) The expression levels of IL-6, IL-1 β , and TNF- α in ox-LDL-induced HUVECs were displayed, with 0 μ g/mL of ox-LDL group as control. (h and i) QPCR and western blot analyses were employed to quantify mRNA and protein levels of α -SMA and SM22- α in HUVECs, respectively. Data shown are mean \pm SD and from three independent experiments. * P < 0.05. Abbreviations: X-inactive-specific transcript (XIST).

3.2 Knockdown of XIST abolished the effects of ox-LDL on proliferation, apoptosis, and inflammatory response of HUVECs

By performing qPCR analysis, we noticed that ox-LDL induced the upregulation of XIST in HUVECs (Figure 2a). The expression level of XIST was decreased in the si-XIST transfected cells than those cells transfected with si-NC (Figure 2b). As presented in Figure 2c, cell viability was increased in ox-LDL-induced HUVECs after knockdown of XIST. In contrast, under ox-LDL condition, HUVECs transfected with si-XIST exhibited fewer apoptotic cells than that in si-NC group (Figure 2d). The western blot analysis revealed that si-XIST significantly decreased the Bax expression, while upregulated Bcl-2 expression in ox-LDL-induced HUVECs (Figure 2e). LDH release was declined in HUVECs treated with si-XIST and ox-LDL than those cells treated with si-NC and ox-LDL (Figure 2f). Moreover, knockdown of XIST significantly weakened

inflammatory response by declining release of IL-6, IL-1 β , and TNF- α in ox-LDL-induced HUVECs (Figure 2g). Additionally, silencing of XIST obviously decreased the expression levels of α -SMA and SM22- α in HUVECs treated with ox-LDL (Figure 2h and i). These results suggested that ox-LDL regulated proliferation, apoptosis, and inflammatory response of HUVECs by upregulating XIST expression.

3.3 XIST negatively regulated miR-98-5p expression in HUVECs

Bioinformatics database Starbase3.0 was used to predict the potential target of XIST. Binding regions between XIST and miR-98-5p, as well as matched mutant sites of XIST-MUT, were displayed in Figure 3a. In addition, the luciferase activity of XIST-WT group was decreased under miR-98-5p overexpression, while XIST-MUT showed

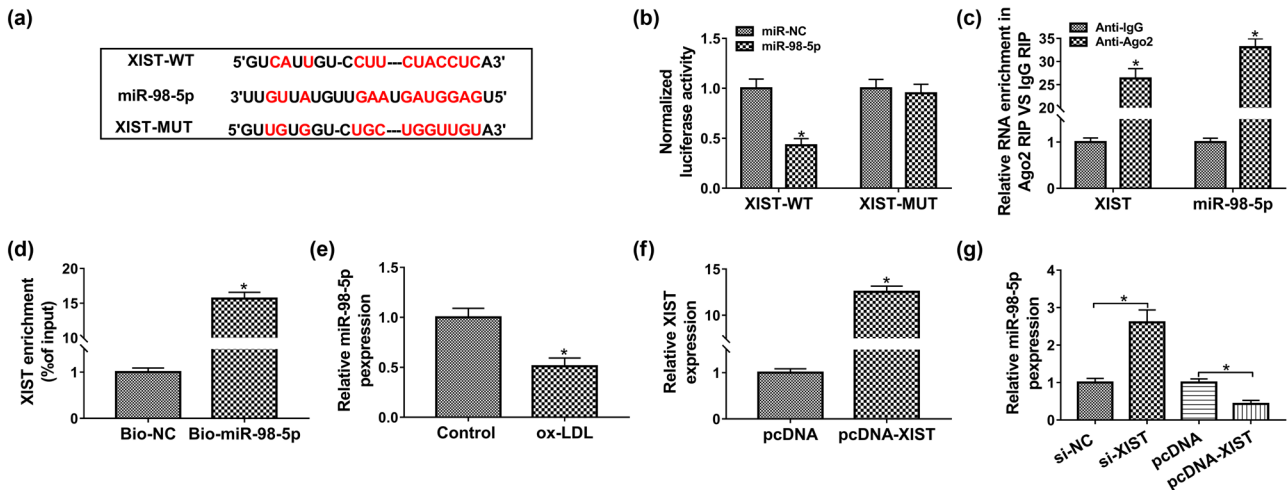


Figure 3: MiR-98-5p was a direct target of XIST. (a) Binding region between miR-98-5p and XIST was predicted by bioinformatics software. (b) Dual-luciferase reporter assay was performed in HUVECs to measure the luciferase activity. (c) After RIP assay, qPCR assay was conducted to assess the enrichments of miR-98-5p and XIST in cell lysates. (d) RNA pull-down assay was used to confirm the association between miR-98-5p and XIST. (e) The expression level of miR-98-5p in HUVECs exposed to ox-LDL was determined by qPCR assay. (f) The transfection efficiency of pcDNA-XIST in HUVECs was checked by qPCR assay. (g) The expression level of miR-98-5p was assessed by qPCR assay in HUVECs transfected with si-NC, si-XIST, pcDNA, or pcDNA-XIST. Data shown are mean \pm SD and from three independent experiments. * $P < 0.05$.

resistance to the impact of miR-98-5p overexpression in HUVECs (Figure 3b). And we also found that Ago2 antibody dramatically enriched XIST and miR-98-5p levels compared to the IgG control by RIP analysis (Figure 3c). After RNA pull-down assay, we noticed that XIST was remarkably enriched in the Bio-miR-98-5p group in comparison with control group (Figure 3d). Moreover, ox-LDL repressed the expression of miR-98-5p in HUVECs (Figure 3e). After transfection with overexpression vector of XIST into HUVECs, we found that XIST was significantly higher in HUVECs transfected with pcDNA-XIST compared with cells transfected with pcDNA (Figure 3f). The functional experiments indicated that silencing of XIST enhanced the expression of miR-98-5p, while overexpression of XIST resulted in opposite results in HUVECs (Figure 3g). Conclusively, XIST regulated miR-98-5p expression in a negative feedback mode in HUVECs exposed to ox-LDL.

3.4 Overexpression of XIST abrogated the upregulation of miR-98-5p-induced effects on proliferation, apoptosis, and inflammatory response in ox-LDL-induced HUVECs

As above results had confirmed that miR-98-5p was a target of XIST, the association between miR-98-5p and

XIST was investigated. MiR-98-5p was overexpressed in HUVECs transfected with miR-98-5p compared with miR-NC group (Figure 4a). The results of MTT analysis revealed that upregulation of XIST weakened the enhancement effect on cell proliferation induced by overexpression of miR-98-5p when HUVECs were exposed to ox-LDL (Figure 4b). Reduction of apoptosis rate induced by miR-98-5p overexpression could be resumed by transfection with pcDNA-XIST into ox-LDL-induced HUVECs (Figure 4c). Western blot assay implied that overexpression of miR-98-5p inhibited Bax, while enhanced Bcl-2 expression in HUVECs treated with ox-LDL, which was overturned by co-transfection with pcDNA-XIST (Figure 4d and e). Next, we performed LDH assay and found that overexpression of miR-98-5p significantly suppressed the LDH release in HUVECs exposed to ox-LDL, which was counteracted by the upregulation of XIST (Figure 4f). The inhibitory effects on IL-6, IL-1 β , and TNF- α expression in ox-LDL-induced cells caused by miR-98-5p mimic were reversed by overexpression of XIST (Figure 4g). Furthermore, upregulation of miR-98-5p impeded the expression of α -SMA and SM22- α , including mRNA and protein, whereas this effect could be abolished by ectopic expression of XIST in ox-LDL-induced HUVECs (Figure 4h and i). Collectively, XIST could strengthen the ox-LDL-induced enhancement effects on apoptosis and inflammatory response, as well as inhibitory effect on proliferation in HUVECs by regulating miR-98-5p.

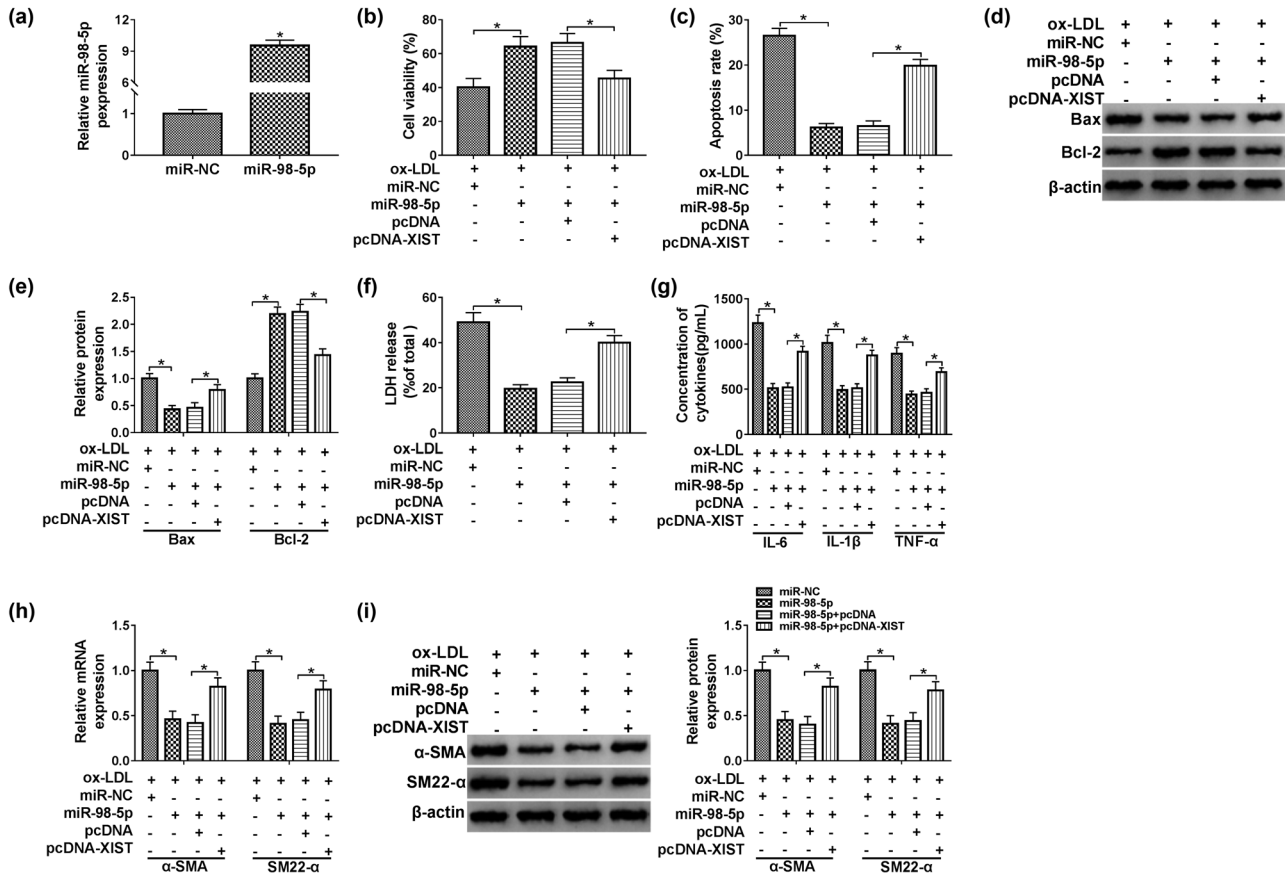


Figure 4: Ox-LDL repressed proliferation and induced apoptosis and inflammatory response in HUVECs by targeting the XIST/miR-98-5p axis. (a) QPCR was enforced to confirm the overexpression efficiency of miR-98-5p in HUVECs. (b–i) HUVECs were treated with ox-LDL + miR-NC, ox-LDL + miR-98-5p, ox-LDL + miR-98-5p + pcDNA, or ox-LDL + miR-98-5p + pcDNA-XIST. (b) MTT assay was used to assess cell viability of HUVECs. (c) Cells apoptosis assay was performed in transfected HUVECs by flow cytometry assay. (d and e) The protein expression levels of Bax and Bcl-2 were calculated in HUVECs by western blot assay. (f) The LDH release was displayed in the different groups by kit assay. (g) The concentrations of IL-6, IL-1 β , and TNF- α in the medium were presented by ELISA assay. (h and i) The mRNA and protein expression levels of α -SMA and SM22- α in HUVECs were detected by qPCR and western blot assays, respectively. Data shown are mean \pm SD and from three independent experiments. * $P < 0.05$.

3.5 PAPPA was a target gene of miR-98-5p in HUVECs

The bioinformatics database analysis suggested that miR-98-5p had the putative binding region in 3'UTR of PAPPA (Figure 5a). The results of dual-luciferase reporter assay indicated that elevated miR-98-5p could decrease the luciferase activity of PAPPA 3'UTR-WT, while luciferase activity of PAPPA 3'UTR-MUT was not changed by miR-98-5p in HUVECs (Figure 5b). Additionally, RIP analysis further verified the specificity of interaction relationship between Ago2 and PAPPA mRNA or miR-98-5p in HUVECs (Figure 5c). More importantly, PAPPA was upregulated in HUVECs exposed to ox-LDL (Figure 5d and e). We also found that miR-98-5p was decreased in HUVECs after transfection with anti-miR-98-5p (Figure 5f).

Moreover, when compared to the control group, the PAPPA expression was suppressed in the miR-98-5p-overexpressing HUVECs, while PAPPA was upregulated by silencing of miR-98-5p in HUVECs (Figure 5g and h). In summary, miR-98-5p negatively regulated PAPPA expression in HUVECs.

3.6 Under ox-LDL condition, knockdown of PAPPA-induced effects on HUVECs could be abolished by silencing of miR-98-5p

The interference efficiency of si-PAPPA was checked by qPCR analysis, and PAPPA was significantly decreased in si-PAPPA group than that in si-NC group (Figure 6a and b).

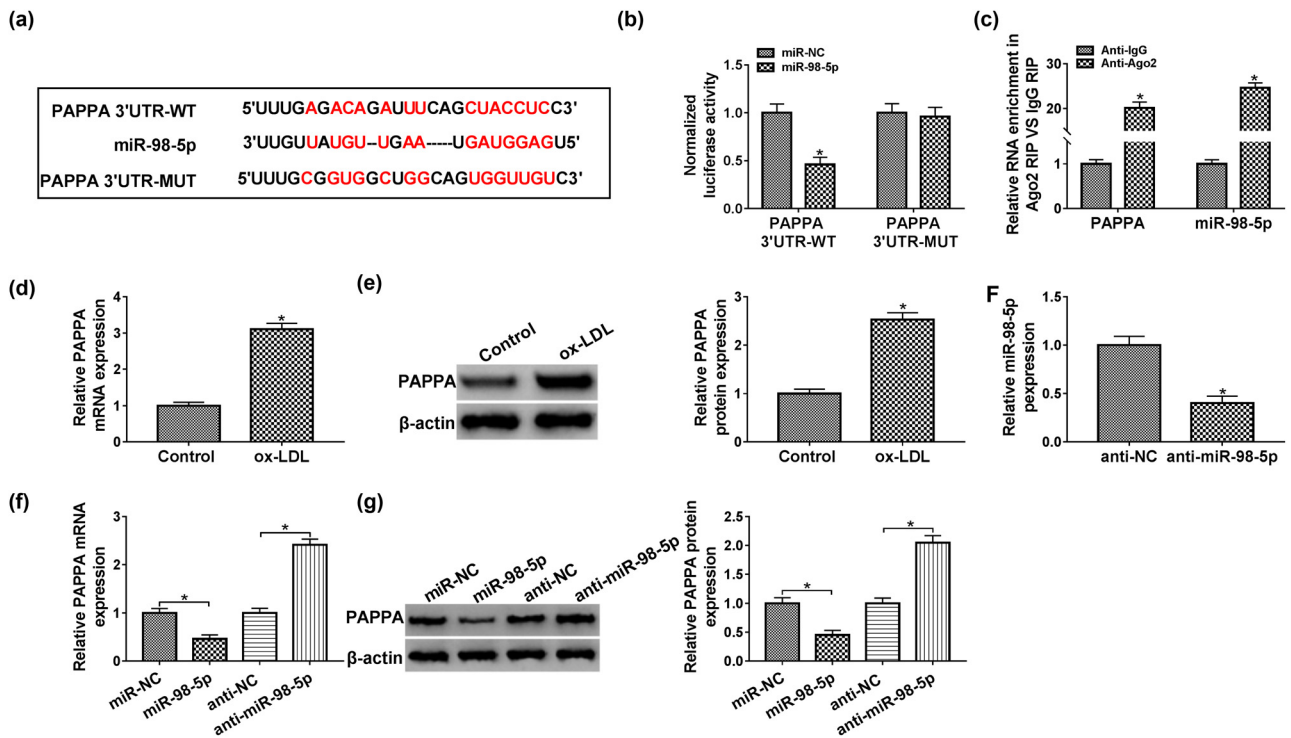


Figure 5: MiR-98-5p negatively regulated PAPP expression in HUVECs. (a) Binding regions between miR-98-5p and PAPP, as well as mutated nucleotides, were shown. (b) HUVECs were co-transfected with indicated luciferase reporter vectors and miR-98-5p mimic or miR-NC for dual-luciferase reporter assay. (c) The expression levels of PAPP and miR-98-5p in Ago2 and IgG group were displayed by RIP assay. (d and e) The mRNA and protein expression levels of PAPP were assessed by qPCR and western blot assay in HUVECs exposed to ox-LDL, respectively. (f) The expression level of miR-98-5p in HUVECs transfected with anti-NC or anti-miR-98-5p was evaluated by qPCR assay. (g and h) QPCR and western blot assays were applied to measure PAPP levels in HUVECs transfected with miR-NC, miR-98-5p, anti-NC, or anti-miR-98-5p. Data shown are mean \pm SD and from three independent experiments. $*P < 0.05$. Abbreviations: pregnancy-associated plasma protein A (PAPP).

MTT assay revealed that cell viability was dramatically upregulated by transfection with si-PAPP, which was partly weakened by transfection of anti-miR-98-5p into ox-LDL-induced HUVECs (Figure 6c). Downregulation of PAPP significantly repressed cell apoptosis, whereas knockdown of miR-98-5p attenuated this change in HUVECs exposed to ox-LDL (Figure 6d). As presented in Figure 6e, silencing of PAPP inhibited Bax, while increased Bcl-2 expression in HUVECs treated with ox-LDL, which was inverted by transfection of miR-98-5p inhibitor into HUVECs. Besides, LDH release in si-PAPP + anti-miR-98-5p group was higher compared with si-PAPP group, indicating that silencing of miR-98-5p promoted LDH release in ox-LDL-induced HUVECs by upregulating PAPP expression (Figure 6f). ELISA analysis revealed that knockdown of PAPP led to downregulation of inflammatory factors including IL-6, IL-1 β , and TNF- α , which was reversed by silencing of miR-98-5p in ox-LDL-induced HUVECs (Figure 6g). It was shown that the mRNA and protein levels of α -SMA and SM22- α were obviously inhibited in

the si-PAPP group compared with si-NC group, while the si-PAPP + anti-miR-98-5p group showed the augmentation of α -SMA and SM22- α expression under ox-LDL condition (Figure 6h and i). Synthetically, above data suggested that ox-LDL regulated proliferation, apoptosis, and inflammatory response in HUVECs by targeting miR-98-5p/PAPP axis.

3.7 XIST increased PAPP expression by regulating miR-98-5p

As shown in Figure 7a and b, the results of qPCR and western blot analyses presented that overexpression of miR-98-5p strikingly declined the expression of PAPP, while this inhibition was abolished by transfecting with pcDNA-XIST into HUVECs. Therefore, PAPP was regulated by XIST/miR-98-5p axis in HUVECs.

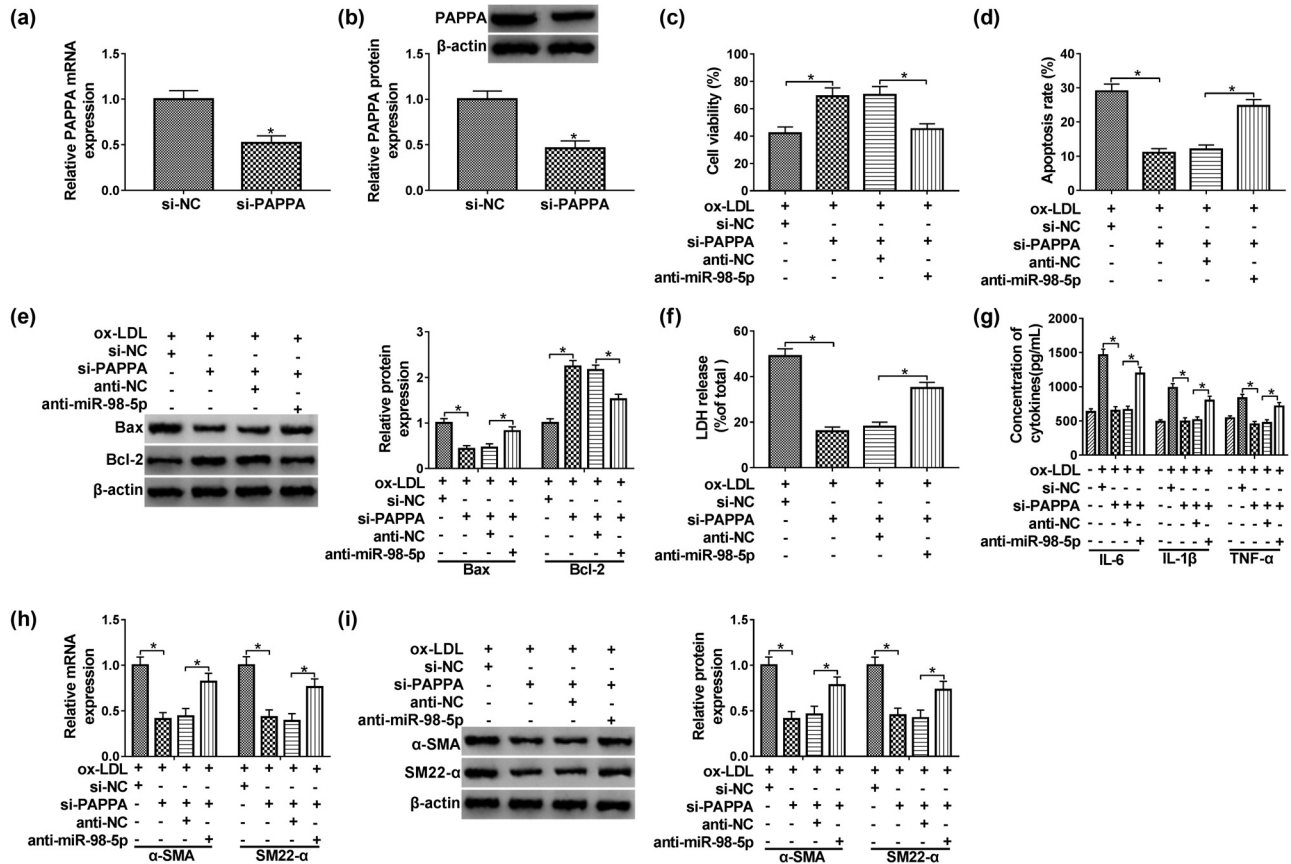


Figure 6: Knockdown of miR-98-5p reversed si-PAPPA induced the effect on proliferation, apoptosis, and inflammatory response in HUVECs. (a and b) The interference efficiency of si-PAPPA in HUVECs was measured using qPCR and western blot assays. (c–f) HUVECs were treated with ox-LDL + si-NC, ox-LDL + si-PAPPA, ox-LDL + si-PAPPA + anti-NC, or ox-LDL + si-PAPPA + anti-miR-98-5p. (c) The cell viability of HUVECs was estimated by MTT assay. (d) Apoptosis analysis was performed in HUVECs using flow cytometry assay. (e) The western blot assay was carried out to analyze Bax and Bcl-2 expression in HUVECs. (f) The LDH detection kit was used to test LDH release in HUVECs. (g) ELISA assay was applied to measure the levels of IL-6, IL-1 β , and TNF- α in the medium, with 0 μ g/mL of ox-LDL group as control. (h and i) The expression levels of α -SMA and SM22- α in HUVECs were assessed by qPCR and western blot assays. Data shown are mean \pm SD and from three independent experiments. * P < 0.05.

4 Discussion

Currently, our results suggested that the cell viability of HUVECs was repressed by ox-LDL in dose/time-dependent method. Consistent with previous research findings [21,22], we also found that ox-LDL could increase HUVECs apoptosis and injury. As we know, HUVECs apoptosis is the key event in the pathogenesis of atherosclerosis [22].

A previous report implied that XIST played a key role in endothelial cell dysfunction [23]. Currently, XIST was overexpressed in HUVECs treated with ox-LDL. Silencing of XIST enhanced proliferation and impeded apoptosis of HUVECs under ox-LDL condition. Similarly, Gu et al. revealed that XIST knockdown protected neuronal cells against spinal cord injury-induced apoptosis [24]. Therefore,

XIST may be a key regulator of survival and apoptosis of endothelial cells.

According to a competing endogenous mechanism, lncRNAs can counteract the role of miRNAs by acting as a sponge for miRNAs [25]. For instance, XIST functioned as a molecular sponge to repress the function of miR-101 in gastric cancer [26]. Our results discovered that miR-98-5p was negatively regulated by XIST and was closely associated with apoptosis, proliferation, and inflammation of ox-LDL-stimulated HUVECs. Mechanistically, XIST elevated the PAPA level by targeting miR-98-5p, which aggravated ox-LDL-induced apoptosis and inflammatory response in HUVECs.

MiRNAs could control gene signaling cascades at post-transcription by binding to target sequences in multiple mRNAs, thereby inducing mRNAs degradation or

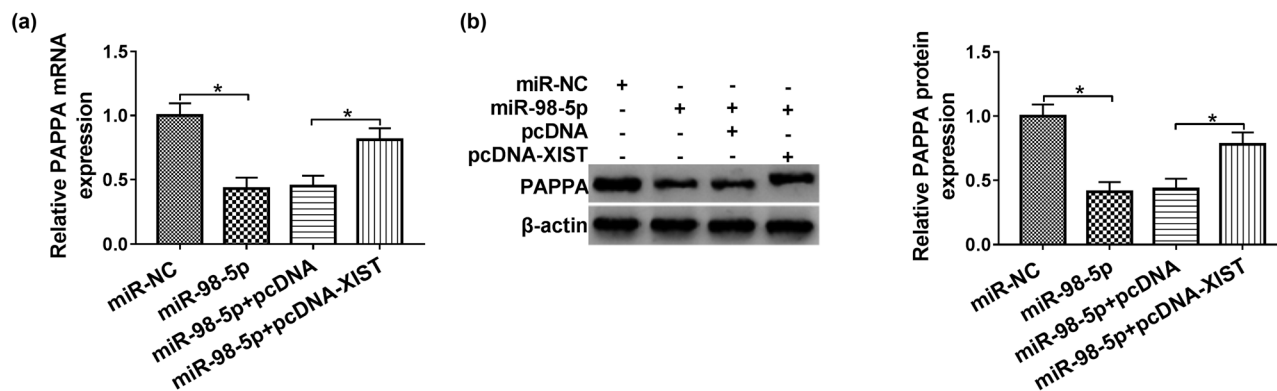


Figure 7: The expression level of PAPP in HUVECs. (a and b) The mRNA and protein expression levels of PAPP in HUVECs transfected with miR-NC, miR-98-5p, miR-98-5p + pcDNA, or miR-98-5p + pcDNA-XIST were examined by qPCR and western blot assays, respectively. Data shown are mean \pm SD and from three independent experiments. * $P < 0.05$.

translational inhibition [27]. MiR-98 has been reported to be connected with cell apoptosis [28]. Chen et al. revealed that miR-98 enhanced the cell growth and extenuated apoptosis of HUVECs exposed to ox-LDL by targetedly inhibiting lectin-like oxidized low-density lipoprotein receptor 1 [29]. As we expected, upregulation of miR-98-5p impeded apoptosis and inflammatory response, as well as upregulated cell viability in HUVECs exposed to ox-LDL; interestingly, upregulation of XIST overturned those effects. Based on these results, miR-98-5p may act as protective roles in vascular disease.

By carrying out bioinformatics database assay and mechanism experiments, PAPP was discovered as a functional target of miR-98-5p in ox-LDL-induced HUVECs. In HUVECs, PAPP induced transcription of tissue factor-mRNA, which may result in formation of intracoronary thrombi and endothelial injury [30,31]. Zhang et al. reported that miR-141 inhibited VSMCs proliferation by targeting PAPP, implying PAPP might play a momentous part in the pathogenesis of atherosclerosis [32]. In addition, Yang et al. confirmed that PAPP was upregulated in human vascular smooth muscle cells under ox-LDL administration [33]. In this study, PAPP was elevated in HUVECs by treatment with ox-LDL. Importantly, silencing of PAPP-induced inhibitory effects on apoptosis and inflammatory response were abolished by transfection with miR-98-5p inhibitor. PAPP was proposed as biomarkers and therapeutic targets for atherosclerosis according to our results.

In a nutshell, the data of our study revealed that downregulation of XIST abolished the ox-LDL-induced effects on HUVECs. Functional experiments provided insight into the function of the XIST/miR-98-5p/PAPP axis in ox-LDL-mediated proliferation, apoptosis, and inflammatory response of HUVECs, which may imply a new molecular biomarker for atherosclerosis.

5 Conclusion

In summary, we found that cell proliferation was inhibited, and inflammation and apoptosis were enhanced in HUVECs by treatment with ox-LDL. Furthermore, XIST was upregulated by ox-LDL in HUVECs. Silencing of XIST increased the cell viability and declined cell apoptosis and inflammation reaction in ox-LDL-stimulated HUVECs. Mechanistically, XIST could directly interact with miR-98-5p, and subsequently acted as a miRNA sponge to regulate the expression of PAPP, which promoted ox-LDL-induced apoptosis, inflammation, and anti-proliferation in HUVECs.

Disclosure of interest: The authors declare that they have no financial conflicts of interest.

Funding: No funding was received.

References

- [1] Qureshi AI, Caplan LR. Intracranial atherosclerosis. *Lancet*. 2014;383(9921):984–98.
- [2] Milutinović A, Šuput D, Zorc-Pleskovič R. Pathogenesis of atherosclerosis in the tunica intima, media, and adventitia of coronary arteries: An updated review. *BJBMS*. 2019;20(1):21–30.
- [3] Zhou Z, Subramanian P, Sevilms G, Globke B, Soehnlein O, Karshovska E, et al. Lipoprotein-derived lysophosphatidic acid promotes atherosclerosis by releasing CXCL1 from the endothelium. *Cell Metab*. 2011;13(5):592–600.
- [4] Pirillo A, Norata GD, Catapano AL. LOX-1, OxLDL, and atherosclerosis. *Mediators Inflamm*. 2013;2013:152786.
- [5] Wu CY, Tang ZH, Jiang L, Li XF, Jiang ZS, Liu LS. PCSK9 siRNA inhibits HUVEC apoptosis induced by ox-LDL via Bcl/

- Bax–caspase9–caspase3 pathway. *Mol Cell Biochem.* 2012;359(1–2):347–58.
- [6] Qin B, Xiao B, Liang D, Xia J, Li Y, Yang H. MicroRNAs expression in ox-LDL treated HUVECs: MiR-365 modulates apoptosis and Bcl-2 expression. *Biochem Biophys Res Commun.* 2011;410(1):127–33.
- [7] Wang KC, Chang HY. Molecular mechanisms of long noncoding RNAs. *Mol Cell.* 2011;43(6):904–14.
- [8] Zhou T, Ding JW, Wang XA, Zheng XX. Long noncoding RNAs and atherosclerosis. *Atherosclerosis.* 2016;248:51–61.
- [9] Li H, Zhu H, Ge J. Long noncoding RNA: recent updates in atherosclerosis. *Int J Biol Sci.* 2016;12(7):898.
- [10] Song P, Ye LF, Zhang C, Peng T, Zhou XH. Long non-coding RNA XIST exerts oncogenic functions in human nasopharyngeal carcinoma by targeting miR-34a-5p. *Gene.* 2016;592(1):8–14.
- [11] Yao Y, Ma J, Xue Y, Wang P, Li Z, Liu J, et al. Knockdown of long non-coding RNA XIST exerts tumor-suppressive functions in human glioblastoma stem cells by up-regulating miR-152. *Cancer Lett.* 2015;359(1):75–86.
- [12] Zhang YL, Li XB, Hou YX, Fang NZ, You JC, Zhou QH. The lncRNA XIST exhibits oncogenic properties via regulation of miR-449a and Bcl-2 in human non-small cell lung cancer. *Acta Pharmacol Sin.* 2017;38(3):371–81.
- [13] Hu C, Bai X, Liu C, Hu Z. Long noncoding RNA XIST participates hypoxia-induced angiogenesis in human brain microvascular endothelial cells through regulating miR-485/SOX7 axis. *Microcirculation.* 2019;11(10):6487–97.
- [14] Madrigal-Matute J, Rotllan N, Aranda JF, Fernández-Hernando C. MicroRNAs and atherosclerosis. *Curr Atheroscler Rep.* 2013;15(5):322.
- [15] Mendell JT, Olson EN. MicroRNAs in stress signaling and human disease. *Cell.* 2012;148(6):1172–87.
- [16] Sun C, Liu H, Guo J, Yu Y, Yang D, He F, et al. MicroRNA-98 negatively regulates myocardial infarction-induced apoptosis by down-regulating Fas and caspase-3. *Sci Rep.* 2017;7(1):7460.
- [17] Li HW, Meng Y, Xie Q, Yi WJ, Lai XL, Bian Q, et al. miR-98 protects endothelial cells against hypoxia/reoxygenation induced-apoptosis by targeting caspase-3. *Biochem Biophys Res Commun.* 2015;467(3):595–601.
- [18] Consuegra-Sanchez L, Fredericks S, Kaski JC. Pregnancy-associated plasma protein-A (PAPP-A) and cardiovascular risk. *Atherosclerosis.* 2009;203(2):346–52.
- [19] You L, Li L, Zhang F, Xu Q, Ren J. A pilot study of the clinical relevance of the relationship between the serum level of pregnancy-associated plasma protein A and the degree of acute coronary syndrome. *J Int Med Res.* 2010;38(2):625–32.
- [20] Wang JL, Li YZ, Tao TQ, Wang XR, Wang Y, Song DD, et al. Postconditioning with calreticulin attenuates myocardial ischemia/reperfusion injury and improves autophagic flux. *Shock (Augusta, Ga).* 2020;53(3):363–72.
- [21] Hong D, Bai YP, Gao HC, Wang X, Li LF, Zhang GG, et al. Ox-LDL induces endothelial cell apoptosis via the LOX-1-dependent endoplasmic reticulum stress pathway. *Atherosclerosis.* 2014;235(2):310–7.
- [22] Zhang Y, Cao Y, You S, Li R, Liu H, Liu C. Protective effects of autophagy against oxidized LDL-induced injury in endothelial cells. *Zhonghua Yi Xue Za Zhi.* 2010;90(39):2792–6.
- [23] Xu X, Ma C, Liu C, Duan Z, Zhang L. Knockdown of long non-coding RNA XIST alleviates oxidative low-density lipoprotein-mediated endothelial cells injury through modulation of miR-320/NOD2 axis. *Biochem Biophys Res Commun.* 2018;503(2):586–92.
- [24] Gu S, Xie R, Liu X, Shou J, Gu W, Che X. Long coding RNA XIST contributes to neuronal apoptosis through the downregulation of AKT phosphorylation and is negatively regulated by miR-494 in rat spinal cord injury. *Int J Mol Sci.* 2017;18(4):732.
- [25] Cheng DL, Xiang YY, Ji LJ, Lu XJ. Competing endogenous RNA interplay in cancer: mechanism, methodology, and perspectives. *Tumor Biol.* 2015;36(2):479–88.
- [26] Chen DL, Ju HQ, Lu YX, Chen LZ, Zeng ZL, Zhang DS, et al. Long non-coding RNA XIST regulates gastric cancer progression by acting as a molecular sponge of miR-101 to modulate EZH2 expression. *J Exp Clin Cancer Res.* 2016;35(1):142.
- [27] Bartel DP. MicroRNAs: Target recognition and regulatory functions. *Cell.* 2009;136(2):215–33.
- [28] Liu X, Cui M. MiRNA-98-5p inhibits the progression of osteosarcoma by regulating cell cycle via targeting CDC25A expression. *Eur Rev Med Pharmacol Sci.* 2019;23:9793–802.
- [29] Chen Z, Wang M, He Q, Li Z, Zhao Y, Wang W, et al. MicroRNA-98 rescues proliferation and alleviates ox-LDL-induced apoptosis in HUVECs by targeting LOX-1. *Exp Ther Med.* 2017;13(5):1702–10.
- [30] Cirillo P, Conte S, Pellegrino G, Ziviello F, Barra G, De Palma R, et al. Pregnancy-associated plasma protein-A promotes TF procoagulant activity in human endothelial cells by Akt–NF-κB axis. *J Thromb Haemost.* 2016;42(2):225–32.
- [31] Roqué M, Reis ED, Fuster V, Padurean A, Fallon JT, Taubman MB, et al. Inhibition of tissue factor reduces thrombus formation and intimal hyperplasia after porcine coronary angioplasty. *J Am Coll Cardiol.* 2000;36(7):2303–10.
- [32] Zhang Y, Chen B, Ming L, Qin H, Zheng L, Yue Z, et al. MicroRNA-141 inhibits vascular smooth muscle cell proliferation through targeting PAPP-A. *Int J Clin Exp Pathol.* 2015;8(11):14401.
- [33] Yang X, Li Z, Zhang L, Wu X, Kang Q, Li L. Knockdown of long non-coding RNA OIP5-AS1 suppresses cell proliferation and migration in ox-LDL-induced human vascular smooth muscle cells (hVMSCs) through targeting miR-152-3p/PAPPa axis. *RSC Adv.* 2019;9(56):32499–509.